HHS Public Access

Author manuscript

J Dairy Sci. Author manuscript; available in PMC 2019 March 24.

Published in final edited form as:

J Dairy Sci. 2018 June ; 101(6): 5531–5548. doi:10.3168/jds.2017-13977.

Metabotypes with elevated protein and lipid catabolism and inflammation precede clinical mastitis in prepartal transition dairy cows

F. Zandkarimi[*], **J. Vanegas**[†], **X. Fern**[‡], **C. S. Maier**[*,§], and **G. Bobe**[§,#,1]

[*]Department of Chemistry, Oregon State University, Corvallis, OR 97331

[†]Department of Veterinary Clinical Sciences, Oregon State University, Corvallis, OR 97331

[‡]Department of Electrical Engineering and Computer Science, Oregon State University, Corvallis, OR 97331

[§]Linus Pauling Institute, Oregon State University, Corvallis, OR 97331

[#]Department of Animal and Rangeland Sciences, Oregon State University, Corvallis, OR 97331

Abstract

Clinical mastitis (CM), the most prevalent and costly disease in dairy cows, is diagnosed most commonly shortly after calving. Current indicators do not satisfactorily predict CM. This study aimed to develop a robust and comprehensive mass spectrometry-based metabolomic and lipidomic workflow using untargeted ultra-performance liquid chromatography high resolution mass spectrometry (UPLC-MS^E) for predictive biomarker detection. Using a nested case-control design, we measured weekly during the prepartal transition period differences in serum metabolites, lipids, inflammation markers, and minerals between clinically healthy Holstein dairy cows that did (MastitisPost; n=8; CM diagnosis day 1: 3 cows, day 2: 2 cows, day 4: 1 cow; day 25: 1 cow, and day 43: 1 cow which had subclinical mastitis since day 3) or did not (Control; n=9) develop CM in early lactation. The largest fold-differences between MastitisPost and Control cows

[1]Corresponding author: Gerd Bobe, 112 Withycombe Hall, Department of Animal and Rangeland Sciences, Oregon State University, Corvallis, OR97331-6702, Phone: 541-737-1898, FAX: 541-737-4174, gerd.bobe@oregonstate.edu.

Supplemental Information

Supplemental Information S1. Animal health surveillance and disease treatment; Supplemental Information S2. Comparison of three sample preparation methods for mass spectrometry analysis of lipids; Supplemental Information S3. Quality control and metabolite and lipid validation; Supplemental Information S4. Data processing and feature annotation; Supplemental Information S5. PLS-DA analyses; Supplemental Information S6. Analytical workflow-Discussion; Figure S1. Total ion chromatograms of serum lipid profiles of the three lipid extraction methods; Figure S2. Principal components analysis (PCA score-plots) generated from the UPLC-MSE analysis of bovine serum lipid extracts of all samples (68 biological samples) and quality control samples (12 pooled QCs); Figure S3. Total serum NEFA concentrations as determined by biochemical and mass spectrometry (MS) analyses; Figure S4. Partial Least Squares - Discriminant Analysis (PLS-DA) plots; Figure S5. Extracted ion chromatograms and tandem mass spectra for sialyllactose isomers; Figure S6. Serum signal intensities of water-soluble phospholipids; Figure S7.Serum signal intensities of free and acylated carnitines; Figure S8. Serum signal intensities of conjugated bile acids; Figure S9.Serum signal intensities of long-chain saturated, monounsaturated, and very long-chain saturated NEFA; Figure S10. Serum signal intensities of unsaturated fatty acids containing LPC; Figure S11.Serum signal intensities of unsaturated fatty acids containing LPE; Figure S12.Serum concentrations of inflammatory markers, lipoprotein markers, metabolites, and minerals measured using biochemical analysis; Figure S13. Body condition score; Table S1.Feed and nutrient composition; Table S2.Reproducibility of commercial diagnostic kits; Table S3. Reproducibility of identified lipid classes in bovine serum; Table S4.Recovery of lipid standards; Table S5. Parameters applied for XCMS and CAMERA; Table S6. List of putatively identified serum metabolites; Table S7.List of putatively identified metabolites that significantly differed between MastitisPost and Control cows; Table S8. List of putatively identified lipids in the bovine serum samples; Table S9.List of putatively identified lipids that significantly differed between MastitisPost and Control cows.

during the prepartal transition period were observed for 3'-sialyllactose in serum. Seven metabolites (*N*-methylethanolamine phosphate, choline, phosphorylcholine, free carnitine, trimethyl lysine, tyrosine, and proline) and 3 metabolite groups (carnitines, amino acids metabolites, and water-soluble phospholipid metabolites) could correctly classify cows for their future CM status at both 21 and 14 days before calving. Biochemical analysis using lipid and metabolite-specific commercial diagnostic kits supported our MS-based omics results and additionally showed elevated inflammatory markers (serum amyloid A and visfatin) in MastitisPost cows. In conclusion, metabolic phenotypes (i.e., metabotype) with elevated protein and lipid metabolism and inflammation may precede CM in prepartal transition dairy cows. The discovered serum metabolites and lipids may assist in predictive diagnostics, prevention strategies, and early treatment intervention against CM, and thereby improve cow health and welfare.

INTERPRETIVE SUMMARY:

To identify risk indicators of clinical mastitis in dairy cows, we compared weekly during the close-up period serum metabolites, lipids, inflammatory markers, and minerals between dairy cows that developed clinical mastitis or remained healthy during early lactation. Seven metabolites and three metabolite groups (carnitines, amino acids and derived metabolites, water-soluble phospholipid metabolites) could correctly classify for future clinical mastitis at 21 and 14 days before calving and thus may assist in predictive diagnostics and early intervention against clinical mastitis.

Keywords

clinical mastitis; lipidomic; metabolomics; transition period; 3'-sialyllactose

INTRODUCTION

Bovine mastitis is an inflammatory response of the mammary gland, which is primarily caused by bacterial infections (Eberhardt, 1996; Viguier et al., 2009). Bovine mastitis can be subdivided into clinical and subclinical mastitis (**CM** and **SCM**): CM can be diagnosed by visible changes in milk consistency and mammary gland appearance (redness, swelling, heat, or pain) or both, and SCM can be diagnosed by elevated SCC in milk (>200,000 cells/mL milk) in the absence of visible changes in milk and udder appearance (Eberhardt, 1996; Sharma et al., 2011). Bovine CM is one of the most prevalent and costly clinical diseases in dairy cows, which makes it economically important to the dairy industry. In the U.S., about 16.5% of the dairy cows have CM in the first 30 days of lactation (USDA, 2009), and the incurred cost is about $440 per case (Kelton et al., 1998; Rollin et al., 2015). Therefore, prevention and early treatment of CM are a priority.

Traditional CM indicator studies focus on indicators in milk at the onset of CM, including SCC counts, serum proteins, enzymes, electrolytes, degradation products of milk proteins, and acute phase proteins (Lai et al., 2009; Sundekilde et al., 2013). In recent years, this research has been extended to metabolomics approaches to discover indicators in infected bovine milk, which can aid in the detection, differential diagnosis of CM based on pathogen, and to examine the pathophysiology of CM (Mansor et al., 2013; Thomas et al., 2016; Xi et al., 2017). Dairy cows are most susceptible to naturally occurring CM within the first weeks

after calving; however, the infection may occur during the close-up period or around calving (Rollin et al., 2015), when milk sample are not available (Hurley and Theil, 2011). Multiple studies have become available during recent years that used blood samples collected during the last two month before and after calving for the discovery of predictive biomarker of various diseases in early lactation dairy cows (Imhasly et al., 2015; Dervishi et al., 2016; Zhang et al., 2017); however, to the best of our knowledge, none looked at predictive serum indicators of CM. Dervishi et al. reported that cows that subsequently developed SCM had 4 weeks before calving elevated serum concentrations of inflammatory markers, monosaccharides, and AA and their metabolites (Dervishi et al., 2015, 2016).

Our hypothesis was that untargeted ultra-performance liquid chromatography high resolution mass spectrometry (**UPLC-MS^{E}**) can be used to discover serum metabolites and lipids that precede CM during the close-up period in dairy cows. To accomplish our goal, our major objectives were: a) to develop a robust and comprehensive, untargeted mass spectrometry-based metabolomic and lipidomic workflow for biomarker detection in serum, which could be also applied to other biological fluids, b) to identify serum metabolites, lipids, minerals, and inflammatory markers, individually or as group, that can classify during the close-up period dairy cows that develop CM in early lactation, and c) to describe temporal changes in serum metabolites, lipids, minerals, and inflammatory markers during the prepartal transition period.

MATERIALS AND METHODS

This study was part of a prospective study designed to identify predictive serum indicators of periparturient diseases in dairy cows. All procedures involving animals were approved by the Oregon State University Institutional Animal Care and Use Committee (ACUP Number 3991).

Study Design and Animal Management

The study cohort consisted of 161 purebred Holstein cows from a 1,000-head commercial dairy farm in Oregon's Central Willamette Valley with 1 to 6 completed lactations that were free of clinical diseases, including abnormal mammary gland appearance (tender, painful or warmth to touch, swelling, hardness, or skin redness), four weeks before expected calving date. Using a nested case-control design, we identified 8 cows that developed CM (**MastitisPost**) and matched them by parity (mean ± SD, range; MastitisPost: 1.88 ± 0.64, 1–3 completed lactations; Control: 1.44 ± 0.73, 1–3 completed lactations), BCS (mean ± SD, range; Control: 3.68 ± 0.19, 3.3–3.9; MastitisPost: 3.75 ± 0.29, 3.3–4.1), and calving season with 9 cows that remained free of clinical diseases (**Control**) as well as subclinical ketosis and hypocalcemia during the first 49 days after calving. CM was diagnosed based on daily test for abnormal milk consistency (e.g., flakes, clots) and mammary gland appearance (redness, swelling, heat, or pain). If abnormal milk consistency, mammary gland appearance, or both were detected, a milk sample was collected and on-farm culturing with blood agar was performed. All MastitisPost cows except two were diagnosed with CM within 4 days after calving: day 1: 3 cows, day 2: 2 cows, and day 4: 1 cow. Another MastitisPost cow had SCM (SCC >1,000,000 cells/mL) directly after calving and was diagnosed with CM 43 days

after calving. The only MastitisPost cow without elevated SCC at the beginning of lactation was diagnosed with CM at 25 days after calving. To identify serum indicators that could precede CM from various naturally occurring pathogens rather than indicators specific to one type of pathogens, we selected cows that differed in pathogens based on cultured growth (gram positive: 3 cows; gram negative: 3 cows; no cultured growth 2 cows). Within one day of CM diagnosis, cows were treated based on their cultured growth. Three MastitisPost cows (6, 9, and 10 month prior) and one Control cow (11 month prior) had an episode of CM in the previous 12 months. Based on the cultured growth, the current CM was from a different pathogen than the prior CM. To avoid confounding with other diseases, cows that developed besides CM other concurrent clinical diseases were excluded from this nested case-control study.

Management of the cows and animal health surveillance and disease treatment has been described in detail previously (Qu et al., 2014); additional information is provided in Supplemental Information S1. Starting 28 days before the expected calving date, BCS of cows were scored once weekly by 3 trained independent evaluators until 4 weeks after calving (Edmonson et al., 1989). Before calving, cows were housed in a straw-bedded free stall barn and were fed once in the morning (7:30 am), a TMR based on corn, corn silage, and alfalfa and triticale hay, which met NRC guidelines (NRC, 2001) as summarized in Table S1. After calving, cows were housed in free stall pens with slatted floors and were fed in head gates around 8:00 and 13:30 a TMR based on corn, corn silage, and alfalfa hay (Table S1), which met NRC guidelines (NRC, 2001).

Sample Collection

Blood samples were taken from the coccygeal vein or artery at 3 weeks (−24 to −18 days), 2 weeks (−17 to −11 days), and 1 week (−10 to −4 days) before calving and the morning after calving within 10 min after morning feeding. We chose serum rather than plasma as biological matrix because of higher metabolite signal intensities with serum than plasma using LC-MS (Yu et al., 2011; Lin et al., 2014), and serum being the preferred biological matrix in recent metabolomic studies in dairy cows (Dervishi et al., 2016; Huber et al., 2016; Zhang et al., 2017). Serum samples were prepared by centrifugation at 1,600 × *g* for 20 min and stored at −80 °C until biochemical, metabolomic, and lipidomic analyses.

Sample Preparation for Mass Spectrometric Analysis

For metabolomic analysis, metabolites were extracted from serum samples by 1:4 dilution with ethanol/methanol (1:1, v/v) as described previously (Kirkwood et al., 2013). Briefly, each sample was vortexed and centrifuged at 16,000 × *g* for 20 min at 4 °C to remove precipitated proteins. Supernatant was transferred to a glass vial for MS analysis.

For lipidomic analysis, three sample preparation methods were initially compared, as described in detail in Supplemental Information S2. The isopropyl alcohol-induced (**IPA**) protein precipitation method was used for all subsequent lipidomic analyses. Lipids were extracted from serum samples by 1:3 dilutions with 240 μL chilled (1:3 v/v) containing non-endogenous lipid standards with final concentrations of 1 mg/L. Each sample was vortex-mixed vigorously for 5 min, and incubated on ice for 10 min. Samples were stored at −20 °C

overnight to enhance protein precipitation. On the following day, each sample was vortex-mixed for 5 min, and centrifuged at 16,000 × *g* for 15 min. Supernatant was transferred to a fresh tube, and stored at −80 °C until MS analysis.

Metabolomic Analysis

Metabolomic analysis was performed by injecting 3 μL of each sample using the flow-through needle mode on Waters Acquity UPLC I class system (Waters, Milford, MA, USA) coupled to a Synapt G2 HDMS mass spectrometer (Waters, Manchester, U.K.). Metabolites were separated on an ACQUITY UPLC BEH amide column (2.1 mm × 150 mm, 1.7 μm, Waters Corporation). Mobile phase A consisted of H_2O/acetonitrile (95:5, v/v), and mobile phase B was H_2O/acetonitrile (5:95, v/v); both mobile phase contained 0.1% formic acid. The following elution gradient was used: 0 min, 99% B; 7.5 min, 40% B; 9 min, 99% B; 10 min, 99% B; 12 min, 99% B. The flow rate was 0.4 mL/min. The temperature of the column compartment was set to 45 °C. The auto-sampler tray was maintained at 6°C. Sample analysis was performed over a 12-min total run time.

The Synapt G2 mass spectrometer was operated in the MS^E mode. All analyses were conducted in both positive and negative electrospray ionization modes. Mass spectral data were acquired from m/z 50 to 1200. A capillary voltage of (±) 2.5 kV and a sampling cone voltage of (±) 35 V were used. Source and desolvation temperature were kept at 100 °C and 400 °C, respectively. Nitrogen was used as desolvation gas with a flow rate of 650 L/hr in the positive ionization mode, and 750 L/hr in the negative ionization mode. Dependent on the ionization mode the protonated molecular ion of leucine enkephalin, $[M+H]^+$ (m/z 556.2771) or the deprotonated molecular ion $[M-H]^-$ (m/z 554.2615) was used as a lock mass for accurate mass measurement. Leucine enkephalin, dissolved in 50% aqueous acetonitrile containing 0.1% formic acid at a concentration of 2 ng/μL, was introduced with a flow rate of 5 μL/min. The lock mass was acquired for 0.3 seconds and repeated every 10 seconds in a separate acquisition channel. In MS^E mode, the low energy function was set to 4 eV in the transfer cell (first function), and for collision induced dissociation the energy in the transfer cell (second function) was ramped from 15 to 35 eV.

Lipidomic Analysis

Lipidomic analysis was performed by injecting 5 μL of each sample using the flow-through needle mode on Waters Acquity UPLC I class system (Waters, Milford, MA, USA) coupled to a Synapt G2 HDMS mass spectrometer (Waters, Manchester, U.K.). Lipids were separated on an Acquity HSS T3 column (2.1 mm × 100 mm, 1.8 μm, Waters Corporation). Mobile phase A consisted of acetonitrile/H_2O (40:60, v/v), and mobile phase B was IPA/acetonitrile/H_2O (85:10:5, v/v/v); both mobile phases contained 10 mM ammonium acetate and 0.1% acetic acid. The following elution gradient was used: 0 min, 40% B; 1 min, 40% B; 11 min, 100% B; 14 min, 100% B, 15 min, 40% B, 16 min, 40% B (1-min for re-equilibration time). The flow rate was 0.4 mL/min. The temperature of the column compartment was set to 55 °C. The auto-sampler tray was maintained at 6°C. Sample analysis was performed over a 15-min total run time. The Synapt G2 mass spectrometer was operated in the data-independent (MS^E) mode using the same settings as described above for

the metabolomic analysis. The exception is that for collision-induced dissociation the energy in the transfer cell (second function) was ramped from 25 to 60 eV.

Detailed information about Quality control (**QC**), metabolite and lipid validation are provided under Supporting Information S3. Detailed information about data processing and feature annotation for lipidomic and metabolomics analysis are provided under Supplemental Information S4.

Biochemical Analysis

Serum concentrations of total glucose, ß-hydroxybutyrate (**BHB**), non-esterified fatty acids (**NEFA**), urea nitrogen, haptoglobin, visfatin, cholesterol, α-tocopherol, calcium, magnesium, and phosphorus were determined as reported previously (Qu et al., 2013; 2014; Fadden and Bobe, 2015). Serum concentrations of serum amyloid A (**SAA**) were determined using a multispecies ELISA kit (Catalog No. KAA0021; Life Technologies, Grand Island, NY), as SAA is highly conserved across species. Manufacturer's instructions were followed for chemical analysis. Absorbance was measured at 450 nm with a FLUOstar Omega microplate auto-reader (BMG Labtech Inc, San Francisco, CA). Serum concentration of serum TNFα was measured with a bovine ELISA kit (Catalog No. RAB0522–1KT; Sigma Aldrich, St. Louis, MO, USA) according manufacturer's instruction. Inter-assay and intra-assay CV are in Table S2.

Data Processing, Statistical Analysis and Self-Organizing Maps

Data acquisition was performed in MassLynx software (version 4.1) in centroid mode. MS data preprocessing and feature extraction were performed using an open-source XCMS package (version 1.39.4) in R (version 3.1.2) environment for peak picking, retention time alignment and filtering as provided under Supplemental Information S4. The area counts for each feature (i.e., signal intensities) in each sample were used for creating bar plots. We performed statistical analyses using MetaboAnalyst, version 2.0 (Xia et al., 2012), GraphPad Prism 7, and SAS version 9.4 (SAS Institute Inc., Cary, NC). For metabolomic data, we normalized area counts for each metabolite in each sample using the Loess algorithm to correct for variations originating from inter-day running differences of the instrument platform (Ejigu et al., 2013). To compare data obtained by biochemical analysis with data obtained by metabolomics or lipidomics, Pearson's correlation coefficient was used.

The potential predictive strength were evaluated by determining how accurately individual serum metabolites and lipids or summed biological families could classify cows for their future CM status. An area under the receiver operating curve (**AUC-ROC**) value of 1 indicates that an individual serum metabolite and lipid or summed biological groups could discriminate between cow groups with 100% accuracy (i.e., complete separation between groups). We also computed AUC-ROC for individual serum metabolites and lipids or summed biological groups that misclassified only one or two cows. We did not compute AUC-ROC for combinations of serum metabolites and lipids, as individual serum metabolites and lipids or summed biological families were sufficient to classify cows.

Significance of differences between MastitisPost and Control cows were evaluated by the nonparametric Wilcoxon rank-sum test. To correct for multiple testing, the Benjamin-Hochberg method was used to compute *q*-values (Broadhurst and Kell, 2007). The results of parametric t-test with Welch-Satterthwaite approximation are not shown because their variance estimates are more susceptible to outliers and violation of normality.

To evaluate differences between MastitisPost and Control cows for the whole data sets (lipidomic, metabolomic, and biochemical data), linear group differences of natural log-transformed, auto-scaled data were calculated and visualized using principal component analysis (**PCA;** unsupervised analysis) and partial least squares discriminant analysis (**PLS-DA**; supervised analysis). Model validation was carried out using a cross-validation test. The goodness of fit ($\mathbf{R^2}$) and predictive power ($\mathbf{Q^2}$) of PLS-DA score plots were calculated.

To evaluate temporal changes within and across MastitisPost and Control cows, a repeated-measures-in-time analysis of natural log-transformed data was conducted in PROC MIXED of SAS. Repeated measures within cows were modeled using a first-order heterogeneous variance-covariance matrix and the Kenward-Rogers approximation was used to adjust the p-values for repeated measures of the same animal. Fixed effects were time (21, 14, 7 days before and directly after calving), group (Control and MastitisPost cows), and their interaction.

To visualize for the whole data sets temporal changes within and across MastitisPost and Control cows, the self-organizing maps (**SOM**) algorithm implemented in Gene Expression Dynamics Inspector (**GEDI**) software was used. For each sampling time, signal intensities of individual lipids from those lipid subclasses were exported into GEDI. Then, 90 (9 × 10) grid coordinates were defined, and trained by using 80 first-phase and 160 second-phase iterations. The resulting heat maps indicate the location of clustered lipids or metabolites as series of coherent mosaic tiles. Because of the small number of measured biochemical parameters (n=11), changes could not be visualized for biochemical data.

RESULTS

Analytical Workflow

The UPLC-MS^E metabolomic and lipidomic analytical workflow for predictive biomarker discovery of bovine CM is summarized in Figure 1A. Using a nested case-control design, we measured serum metabolites, lipids, inflammatory markers and minerals at −21, −14, −7, and 0 days from cows that in early lactation did or did not develop CM. The extracted serum metabolites and lipids were separated using hydrophilic interaction liquid chromatography (**HILIC**) and Reversed-phase UPLC, respectively, and detected and quantified by high resolution MS^E and ion-mobility spectrometry ion-mobility spectrometry-mass spectrometry (**IMS-MS^E**). We used the XCMS-package in R for data extraction and preprocessing as summarized in Figure 1B. We applied parametric and non-parametric approaches to classify cows for future CM and determine dynamic changes within and across groups, which were visualized using linear and non-linear clustering methods. We utilized on-line databases for tentative identification of features. Mass spectrometry-based omics was complemented by biochemical assays for clinical diagnostics and validation of MS-derived findings.

Within the analytical workflow, we tested 3 lipid extraction/precipitation methods: two lipid-liquid extraction methods, methanol/methyl tert-butyl ether and dichloromethane/methanol, and one protein precipitation method with IPA (Supplemental Information S2). We were able to extract the major lipid classes and subclasses with all three methods (Figure S1); the total numbers of extracted features for each of the tested protocol were around 2,250 and 1,450 ions in the positive and negative modes, respectively. The three extraction methods, however, resulted in differences in signal intensities for NEFA (negative mode), triacylglycerol (**TAG**), and cholesteryl esters (**ChoE**) (both in positive mode) with the IPA precipitation yielding the highest ion intensities for NEFA, TAG, and ChoE (Figure S1). The IPA method was used for all subsequent lipidomic analyses and provided satisfactory recovery and reproducibility CV (both <12%) for all the major lipid classes and subclasses (Figure S2; Tables S3, S4). For validation of our lipidomic workflow, we compared results of the summed signal intensities of individual NEFA with the total NEFA results using the biochemical, colorimetric method. As shown in Figure S3, results for summed signal intensities of individual NEFA using MS were in close agreement with the NEFA results using the biochemical, colorimetric method for the 68 examined samples, as exemplified by the Pearson correlation of $r = 0.91$ and $R^2 = 0.84$. Further details and the discussion about the analytical workflow are provided under Supplemental Information.

Serum Metabolite Differences between MastitisPost vs. Control Cows

A total of 2,200 features were detected in both LC-ESI-MS^E positive and negative modes combined during a 12-min retention time window. We annotated putatively 81 unique molecular metabolites to be 17 proteinogenic AA, 16 AA metabolites, 4 dipeptides, 15 carnitines (**Car**), 7 bile acids (**BA**), 6 water-soluble phospholipid (**PL**) metabolites, 6 carbohydrates, 4 nucleotides and nucleotide metabolites, 3 cholesterol and ChoE, 2 vitamins, and 1 sphingosine metabolite (Table S6). Linear, supervised multivariate analysis of extracted metabolite features from the negative mode displayed distinct clustering and clear separation of MastitisPost and Control cows at each sampling time (Figure S4A).

Of the 81 metabolites, 17, 7, 0, and 1 could correctly classify for future CM of cows (AUC-ROC = 1) at −21, −14, −7, and 0 days, respectively (Table 1). Each metabolite was higher before calving in MastitisPost vs. Control cows, and median fold-changes of each metabolite decreased as calving approached. Each of the 7 metabolites, *N*-methylethanolamine phosphate (**MEP**), choline, phosphorylcholine, free carnitine, trimethyl lysine (**TML**), tyrosine, and proline, that could correctly classify for future CM at −14 d could also do so at −21 d. Summed signal intensities of AA metabolites, water-soluble PL metabolites, and carnitines could correctly classify for future CM of cows (AUC-ROC = 1) at both −21 and −14 days.

Significant ($p < 0.05$) group differences between MastitisPost and Control cows were observed at all 4 sampling time for two metabolites, 3'-sialyllactose (**3'-SL;** Figure 2A) and glycodeoxycholic acid (**GDCA**) (Table 1); the presence of both was confirmed by comparison with commercial standards and fragmentation patterns (Figure S5 for 3'SL). Five additional metabolites, lactose, betaine, free carnitine, Car C3:0, Car C18:1, and proline, differed at −21, −14, and −7 days (all higher in MastitisPost vs. Control cows), as

did summed signal intensities of AA metabolites (Figure 2B), carnitines (Figure 2C) and water-soluble PL metabolites (Figure 2D). Three additional metabolites, hippuric acid, taurocholic acid (**TCA**), and glycocholic acid (**GCA**), were higher in MastitisPost vs. Control cows at −21 and −14 days and lower at 0 days, as did summed signal intensities of conjugated BA (Figure 2E). The largest fold-changes before calving among all metabolites and lipids were observed for the mammary-gland derived carbohydrates 3'-SL and lactose (Table 1), which showed similar temporal group differences (Figure 2A).

Before calving, 5 metabolite families, AA metabolites, proteogenic AA (Figure 2B), water-soluble PL, carnitines, and conjugated BA, had over half of the individual metabolites with higher signal intensities in MastitisPost vs. Control cows: 14, 11, and 2 of 16 identified AA metabolites; 5, 6, and 4 of 6 identified water-soluble PL; 9, 9, and 7 of 15 identified carnitines; and 4, 3, and 1 of 5 identified conjugated BA were higher in MastitisPost vs. Control cows at −21, −14, and −7 days, respectively. The largest group differences of individual metabolites were observed at −21 days and the smallest at −7 days.

At calving, serum metabolites were either lower in MastitisPost vs. Control cows or similar. Of the 14 metabolites that differed, 11 were lower. Those included all 5 identified conjugated BA individually (Figure S8) as well as their summed signal intensities (Figure 2E). The remaining metabolites that differed at calving in MastitisPost vs. Control cows were distributed over all metabolite families: lower were one conjugated BA precursor (glycine), one water-soluble PL metabolite (glycerylphosphoethanolamine), one AA metabolite carrier (Car C5:0), and two AA metabolites (hippuric acid, indoxylsulfate) and higher were one AA (histidine), one AA metabolite (ketoleucine) and 3'-SL.

Serum Lipid Differences between MastitisPost vs. Control Cows

A total of more than 2,200 features were detected in both LC-ESI-MS^E positive and negative modes combined during a 15-min retention time window. We annotated putatively 204 individual molecular lipids to be 41 phosphocholine (**PC**), 24 phosphoethanolamine (**PE**), 10 phosphoinositol (**PI**), 21 phosphoserine (**PS**), 19 sphingomyeline (**SM**), 12 lysophosphocholine (**LPC**), 10 lysophosphoethanolamine (**LPE**), 1 lysophosphoinositol (**LPI**), 2 diacylglycerols (**DG**), 23 TAG, 4 ChoE, 12 ceramides (**Cer**), and 24 NEFA (Table S8). Supervised, linear, multivariate analysis on the extracted lipidomic features from the negative mode depicts distinguishable clustering of Control and MastitisPost cows at each sampling time (Figure S4B). However, none of the individual lipids or lipid families could correctly classify for future CM status of cows (AUC-ROC = 1). The best lipid discriminator was the relative proportion of NEFA on total FA (NEFA%), which could correctly classify at calving for future CM status of cows except for the only MastitisPost cow that had normal SCC at the onset of lactation (Figure 3A). The only two lipids that had significant differences in signaling intensities at ≥3 sampling times were PC(16:0/16:1) and TAG (16:0/18:0/18:1) (Table 1).

At −21 days, 23 lipids differed (all $p < 0.05$) between MastitisPost and Control cows. Summed signal intensities of esterified FA (sum of FA of Cer, TAG, DG, LPC, LPE, LPI, PC, PE, PI, PS, and SM; +23%) were higher ($p = 0.04$) in MastitisPost vs. Control cows (Figure 3A); this was primarily due to higher signal intensities of the most abundant

esterified FA, PC (+35%; Figure 3B) and UFA containing TAG (+24%; Figure 3B). Moreover, the ratio of 18:1 to 18:0 FA (C18 desaturase index) in TAG was higher (+57%) in MastitisPost vs. Control cows. In contrast, summed signal intensities of very long-chain SFA (20:0 to 28:0; −45%) and *N3*-PUFA (18:3, 20:5, 22:5; -−33%) were lower (all $p < 0.05$) in MastitisPost vs. Control cows at −21 days before calving (Figure 3C). As calving approached, less lipid ions differed between MastitisPost vs. Control cows (11 at −14 days and 12 at −7 days).

At calving, the largest number (i.e. 59) of lipids differed between MastitisPost vs. Control cows (Table S9). Summed signal intensities of NEFA (+121%) were higher ($p = 0.01$) in MastitisPost vs. Control cows (Figure 3A), which was primarily due to the higher signal intensities of the most abundant NEFA, long-chain SFA (+112%; $p = 0.02$) and MUFA (+182%; $p = 0.005$) (Figure 3C). Signal intensities of each identified long-chain and monounsaturated NEFA was higher in MastitisPost vs. Control cows. In contrast to long-chain NEFA, summed signal intensities of very long-chain SFA (−23%; $p = 0.007$), PC (−19%; $p = 0.03$; Figure 3B), PI (−26%; $p = 0.02$; Figure 3B), 18:0-containing TAG (−53%; $p = 0.02$), monohexosylCer (−29%; $p = 0.04$), and summed signal intensities of UFA-containing LPC (−46%; $p = 0.007$), LPE (−42%; $p = 0.01$), and ChoE (−41%; $p = 0.004$) were lower in MastitisPost vs. Control cows (Figure 3D). Moreover, the ratio of UFA-containing LPE to PE (−65%; $p < 0.0001$, complete group separation) and the ratio of UFA-containing LPC to PC (−17%; $p < 0.03$) was lower in MastitisPost vs. Control cows, whereas the ratio of 18:1 to 18:0 FA (C18 desaturase index) in TAG was higher (+274%; $p < 0.007$).

Serum Biochemical Differences between MastitisPost vs. Control Cows

For biochemical analysis, we quantified serum concentrations of markers of acute and chronic inflammation (haptoglobin, SAA, TNFα, visfatin; Figure S12A), lipoprotein metabolism (α-tocopherol, cholesterol; Figure S12B), energy status (NEFA, BHB, glucose, urea N; Figures S12C), and mineral status (calcium, magnesium, phosphorus; Figure S12D). In addition, we measured BCS at each sampling time (Figure S13). PLS-DA score plots showed distinct clustering of MastitisPost and Control cows at each sampling time except at 14 days before calving (Figure S4C).

Separation between MastitisPost and Control cows was driven by SAA, visfatin, and α-tocopherol. Whereas markers of inflammation were higher in MastitisPost vs. Control cows throughout the sampling period, serum concentrations of α-tocopherol were lower (Table 1). Complete group separation were observed for visfatin at −7 and 0 days. Significant group differences at all 4 sampling times were observed for visfatin and α-tocopherol and at the last 3 sampling times for SAA and summed concentrations of inflammatory markers (Figure 4).

Similar to the results obtained with MS, serum concentrations of total NEFA were higher ($p \leq 0.05$) in MastitisPost vs. Control cows at −7 days (+139%) and 0 days (+178%). Higher serum concentrations of haptoglobin were not observed in MastitisPost vs. Control cows until after calving (0 days: +251%; results after calving not shown). Other indicators and indicator families showed no or limited ability to predict CM and differed ($p \leq 0.05$)

between MastitisPost and Control cows at only 1 (glucose, phosphorus) or 0 sampling times (BHB, calcium, cholesterol, magnesium, urea N, TNFα, BCS).

Temporal Serum Metabolite and Lipid Changes during the Prepartal Transition Period

Temporal serum metabolite changes during the prepartal transition period were visualized using SOM in GEDI. For metabolomics results, GEDI grouped carnitines, AA and their metabolites, and conjugated BA in distinct and separate tiles (Figure 5A). Temporal metabolite changes differed between metabolite families as well as between MastitisPost and Control cows. Larger decreases in summed signal intensities were observed in MastitisPost vs. Control cows for AA (−60% vs. −34% Figure 2B) and AA metabolites (−46% vs. −22%; Figure 2B), free Car (−91% vs. −69%; Figure 2C), and water-soluble PL (−91% vs. −69%; Figure 2D), all of which primarily decreased between −14 and −7 days. Summed signal intensities of acylated carnitines (Control cows: +6%, $p = 0.56$; MastitisPost cows: −52%, $p < 0.0001$, primary decrease between −14 and −7 days; Figure 2C) and conjugated BA (Control cows: +37%, $p = 0.33$; MastitisPost cows: −87%, $p < 0.0001$, consistent decrease throughout; Figure 2E) only decreased in MastitisPost cows.

For the lipidomics results, GEDI grouped NEFA, TAG, PC, LPC & LPE, and PE in distinct and separate tiles (Figure 5B). Temporal metabolite changes differed between metabolite families as well as between MastitisPost and Control cows. During the prepartal transition period, cows transitioned from lipid synthesis to lipid catabolism. Relative abundance of NEFA increased exponentially starting −7 days, whereas the relative abundance of esterified FA, including TAG, LPC & LPE, and PC, decreased until calving. Larger temporal changes were observed in MastitisPost vs. Control cows: the proportion of NEFA on total FA (NEFA %) increased stronger in MastitisPost vs. Control cows (+333% vs. +82%; $p = 0.02$; Figure 3A), as summed signal intensities of NEFA (MastitisPost vs. Control cows: +338% vs. +89%; Figure 3A) and summed signal intensities of LPC (−59% vs. −39%), PC (−49% vs. −15%), PE (−24% vs. +5%), and PI (−26% vs. +36%) changed in opposite directions; the change being significant only in MastitisPost cows. Summed signal intensities of PS, LPE, SM, monohexosylCer, and ChoE as well as cholesterol decreased similarly in both groups during the prepartal transition period.

Integrative Overview of Dynamic Changes during the Prepartal Transition Period

Dynamic changes of metabolites, lipids, and inflammatory markers during the prepartal transition period are linked and integrated in Figure 6 to provide a schematic representation of our study results. At −21 days (Figure 6A), serum markers of muscle protein breakdown (AA and their metabolites, odd short-chain acyl carnitines), muscle and liver FA oxidation (long-chain acyl carnitines), chronic inflammation (visfatin), liver choline metabolism (water-soluble PL metabolites), mammary gland development (mammary gland-derived carbohydrates), and liver lipid synthesis, packaging, secretion, and recycling (conjugated BA, PL, TAG) were higher in MastitisPost vs. Control cows. Whereas group differences between serum metabolites decreased until calving except for markers of early mammary gland development, signal intensities of serum markers of acute inflammation (SAA) and adipocyte TAG breakdown (long-chain saturated and monounsaturated NEFA) increased in MastitisPost cows starting at −14 days but not in Control cows before calving. At calving

(Figure 6B), serum markers of acute and chronic inflammation (SAA, visfatin) and adipocyte TAG breakdown catabolism (long-chain SFA and MUFA) were higher and markers of liver lipid synthesis, packaging, secretion and recycling as well as intestinal lipid absorption and synthesis (esterified FA, PC, PI, C18:0 containing TAG, unsaturated LPC, LPE, and ChoE, and conjugated BA) were lower in MastitisPost vs. Control cows at calving.

DISCUSSION

The last three weeks before calving, also called prepartal transition period, is marked by homeorhetic metabolomic and lipidomic adaptations for the upcoming parturition and lactation, which are orchestrated by hormonal changes (Drackley, 1999; Ingvartsen, 2006). Reasons for these adaptations include: exponentially increasing energy, amino acid, and lipid requirements for the growing fetus and expanding mammary gland; accumulation of minerals and vitamins, growth factors, antioxidants, immunoglobulins and bactericidal compounds in the colostrum to strengthen immune-response of the immune-naïve neonate. In addition, fetus size may limit rumen size and, thus, feed intake. During the transition period, immunosuppression results in increased susceptibility to infectious diseases such as CM. Given this physiological background, the objective of this study was to identify predictive indicators that precede CM in dairy cows.

Metabotype Differences between MastitisPost and Control Cows at −21 and −14 Days

Elevated signal intensities of multiple serum AA and AA metabolites and carnitines were observed in MastitisPost cows at −21 and −14 days. Carnitine and AA metabolism are linked as the breakdown of endogenous proteins containing TML residues is recognized as the starting point for free carnitine synthesis (Servillo et al., 2014). Acylated carnitines play important roles in both AA oxidation, specifically short-chain odd acylcarnitines (Car C3:0 and CarC 5:0), and FA β-oxidation, specifically long-chain even acylcarnitines in muscle and liver (Koves et al., 2008). Medium-chain acylcarnitines (Car C10:0) indicate incomplete FA β-oxidation, when NEFA availability exceeds the amount that can be oxidized in the mitochondria. Elevated AA and AA metabolites and carnitines have been reported by the Ametaj research group 8 or 4 weeks prepartum in cows, which were diagnosed postpartum with various diseases, including SCM (Hailemariam et al., 2014; Dervishi et al., 2016; Zhang et al., 2017). The Ametaj group proposed that inflammation was the cause of the observed metabolic changes. For example, elevated concentrations of serum haptoglobin, TNFα, and IL-1 preceded SCM diagnosis 4 weeks prepartum (Dervishi et al., 2015).

To evaluate whether inflammation associated with infection may have triggered the MastitisPost metabotype observed at −21 days, we measured serum markers of chronic (visfatin) and acute inflammation (SAA, haptoglobin, TNFα). Visfatin but not markers of acute inflammation were elevated in MastitisPost vs. Control cows. We checked also for previous SCC and mastitis events of MastitisPost cows, and the results indicated that MastitisPost cows were most likely free of mammary infections at −21 days. Thus, chronic inflammation may precede AA and FA catabolism, which may cause those cows to be more susceptible to mammary infections (Sordillo et al., 2009).

One question arises whether the elevated AA and FA catabolism can be explained by decreased feed intake rather than inflammation. The answer is not straightforward, as there is a synergistic interrelation between inflammation, decreased feed intake, and elevated AA and FA catabolism. Inflammation-associated cytokine and hormone release decreases feed intake and increases protein and lipid catabolism in liver and muscle; however the reverse is also true (Kuhla et al., 2011; Sordillo et al., 2009). Thus, the question becomes what happened first: inflammation, the AA and FA catabolic metabolic phenotype (i.e. **metabotype**), or low feed intake. We cannot answer this question, as chronic inflammation and the AA and FA catabolic metabotype both were evident at −21 days. A limitation for the interpretation of our data is that we did not measure feed intake; however, we can utilize NEFA, BHB, and BCS as indicator of energy status (Moyes et al., 2013), and neither differed between MastitisPost and Control cows at −21 and −14 days. We propose that cows develop as they age a chronic inflammatory metabotype (i.e., “inflammaging”), similar to what has been proposed in the human literature (Franceschi et al., 2007). Besides chronic inflammation, hallmarks of inflammaging is progressive mitochondrial dysfunction, as indicated by elevated AA and FA catabolism, and increased reactive oxygen species accumulation and cellular damage (López-Otin et al., 2013), which may be the cause of low serum concentrations of α-tocopherol in MastitisPost cows. In support of our proposed mechanism, Huber et al. (2016) observed in early lactation dairy cows that later failed to conceive an inflammatory metabotype with mitochondrial dysfunction, which was not linked to decreased feed intake.

Whereas Huber et al. (2016) and recent Ametaj group studies used a targeted metabolomics approach, our untargeted metabolomic and lipidomic study allowed us to look at a broader number of metabolite and lipid families (e.g., BA and water-soluble PL). At −21 and −14 days, elevated levels of conjugated BA were observed in MastitisPost cows. Our results for conjugated BA are similar to those observed in human pregnancy-associated cholestasis, in which pregnancy hormones stop or slow down bile flow, resulting in a build-up of BA in the liver that spills in the blood stream (Lammert et al., 2000; Geenes and Williamson, 2009). Our observed elevated PC levels at −21 days may be related to the elevated conjugated BA levels indicating pregnancy-associated cholestasis. Decreased bile flow, as indicated by elevated conjugated BA concentrations, may interfere with hepatic removal of pathogens and their toxic products. Future studies are warranted to examine whether pregnancy-associated cholestasis is a health problem in dairy cows.

At −21 and −14 days, nearly all water-soluble PL metabolites were elevated in MastitisPost vs. Control cows. In humans, pregnancy (i.e., increased choline transfer into the fetus) as well as various diseases (e.g., coronary heart disease) are associated with elevated circulating choline concentrations (Danne et al., 2007; Yan et al., 2012). The likely reason is that high needs for methyl groups of fast-growing and metabolizing tissues (i.e., nucleotide synthesis, methylation) and high choline and betaine excretion results in elevated choline metabolism (Yan et al., 2012; Ducker and Rabinowitz, 2017). Carnitine, AA and AA metabolites, and water-soluble PL metabolites are metabolically linked, as choline via betaine provides methyl groups for carnitine biosynthesis (Griffith, 1987; Zhou et al., 2017), which is essential for AA and FA metabolism. Thus, elevated serum levels of water-soluble

PL metabolites may indicate both inflammation-associated diseases and elevated AA and FA catabolism in muscle and liver.

One of the most intriguing observations from a physiologic perspective involved summed signal intensities of esterified FA (sum of FA of Cer, DG, LPC, LPE, LPI, PC, PE, PI, PS, SM, and TAG). At −21 days, summed signal intensities of esterified FA were higher in MastitisPost vs. Control cows, which was primarily due to higher signal intensities of the most abundant esterified FA-containing lipid ions, PC and TAG containing 18:1, 18:2, or both. Circulating TAG are primarily associated with VLDL, and TAG's FA composition mainly reflects hepatic lipid metabolism and secretion (Gray et al., 2013). We interpret our observation as indication of elevated hepatic lipid biosynthesis and VLDL secretion in MastitisPost vs. Control cows. Stearoyl-CoA desaturase is the rate-limiting enzyme in MUFA synthesis and critical for both hepatic lipid biosynthesis and VLDL secretion (Stefan et al., 2008). We observed higher 18:1 to 18:0 FA ratios (i.e., C18 desaturase index) in TAG of MastitisPost vs. Control cows at −21 days, suggesting greater hepatic stearoyl CoA desaturase activity in MastitisPost vs. Control cows. In humans, greater hepatic stearoyl CoA desaturase 1 activity is related to more VLDL secretion and less liver fat but also to increased hepatic lipid synthesis and less hepatic FA oxidation (Stefan et al., 2008; Silbernagel et al., 2012). Thus, MastitisPost cows may differ from Control cows in endogenous lipid metabolism (i.e., higher stearoyl CoA desaturase activity).

Summed signal intensities of two NEFA subfamilies, *N3* PUFA and very long-chain SFA, were lower in MastitisPost vs. Control cows at −21 days. Serum *N3* PUFA are known to have anti-inflammatory properties (Tai and Ding, 2010). Lower circulating concentrations of very-long chain SFA, which have important roles in membrane structure and intracellular signaling, are associated with increased risk of chronic diseases in humans (Lee et al., 2015; Malik et al., 2015). We are not aware of studies examining the relation between circulating very long-chain SFA, their synthesis and degradation, and bovine diseases, indicating an area of future research.

Consistent Metabotype Differences between MastitisPost and Control Cows

The most consistent single discriminant metabolite in our data was 3'-SL followed by lactose; both metabolites are synthesized exclusively in the mammary gland. Sialyllactose is the smallest acidic oligosaccharide and most abundant oligosaccharide in bovine milk (>50% of oligosaccharides) and occurs in two isomeric forms 3'-SL and 6'-SL (Gopal and Gill, 2000); 3'-SL is more abundant in bovine milk than 6'-SL, which is the major SL in human milk (Nakamura et al., 2003; Tao et al., 2009; Ten Bruggencate et al., 2014). We detected and validated the presence of 3′-SL and 6'-SL by comparing the serum samples with commercial standards, and we only could detect 3′-SL in our serum samples. The proposed function of 3'-SL and 6'-SL is to protect calves against infections (Nakamura et al., 2003) and to support innate immunity in newborns (Ten Bruggencate et al., 2014); thus 3'-SL may be increased during an infection. Both, 3'-SL and lactose, increased during the prepartal transition period in Control cows, whereas their values were already elevated at −21 days in MastitisPost cows, indicating earlier mammary gland development in MastitisPost cows. We excluded delayed calving as potential explanation for earlier

mammary gland development because pregnancy length did not significantly differ between MastitisPost and Control cows ($p = 0.12$). Elevated 3'-SL and lactose in serum of MastitisPost cows may indicate passive transfer of mammary gland-derived compounds into serum as a result of pathogen-induced damage of the mammary gland epithelial barrier between blood and milk (MacKenzie and Lascelles, 1968). It is intriguing that a mammary gland-derived oligosaccharide in serum may assist in CM prediction, given that several blood-derived metabolites in milk are used as indicators of CM (Viguier et al., 2009). Further studies are required to validate and quantify this proposed metabolite as a robust predictive indicator of CM and potentially SCM.

Serum visfatin concentrations were elevated and serum α-tocopherol concentrations were lower in MastitisPost vs. Control cows throughout the prepartal transition period. This is similar to what we previously reported in dairy cows that subsequently developed retained placenta and other diseases (Qu et al., 2013, 2014; Fadden and Bobe, 2015), indicating chronic inflammation and depleted antioxidant reserves are potential risk factors of CM. .

Metabotype Differences between MastitisPost and Control Cows at Calving

Metabotype differences started to change between −14 and −7 days. There was a shift from elevated AA and FA oxidation to increased adipose lipolysis in MastitisPost cows, which may relate to the decrease in carnitine levels and depleted carnitine stores for FA and AA oxidation. We propose that the shift is the result of an acute infection, as indicated by increased SAA concentrations in MastitisPost cows, suggesting that during this time period MastitisPost cows became infected with CM. The SAA increase preceded the increase in long-chain SFA and MUFA, which are FA enriched in adipose tissue (Rukkwamsuk et al., 2000), indicating that acute inflammation most likely caused adipose lipolysis. This sequence of events had been reported in metabolomics studies for other postpartum diseases (Hailemariam et al., 2014; Dervishi et al., 2015; 2016).

Novel findings are the lower serum conjugated BA levels in MastitisPost vs. Control cows directly after calving, which may indicate decreased intestinal lipid absorption and bile recycling postpartum. This could also explain the lower PL levels of MastitisPost vs. Control cows at calving. Lower serum BA levels may also explain in part the higher acute phase protein concentrations in MastitisPost vs. Control cows after calving, because lower BA concentrations may result through less farnesoid X receptor (FXR) activation in more proinflammatory cytokine synthesis and inflammation (Wang et al., 2008).

Also novel were the lower signal intensities of esterified FA, PC, PI, C18:0 containing TAG, unsaturated LPC, LPE, and ChoE in MastitisPost vs. Control cows at calving. As a consequence, the proportion of NEFA on total FA (NEFA%) was 2-fold higher in MastitisPost vs. Control cows with complete separation of groups except for the only MastitisPost cow that was without disease directly after calving. This makes biologically sense, as NEFA% accounts not only for the increased NEFA release from adipose tissue but also for the decreased esterified FA release from the liver in sick cows. Inadequate PC and PI availability has been implicated in decreased hepatic lipoprotein assembly and lipid secretion in transition dairy cows (Bobe et al., 2004). Serum ChoE are synthesized in serum high-density lipoproteins (HDL) by transacylation of PC, a reaction that is inhibited by

inflammation (Kontush et al., 2013; Kessler et al., 2014). Our results are consistent with a cytokine-induced decrease in hepatic lipoprotein secretion in response to an acute mammary infection (Gruys et al., 2005; Bannerman et al., 2009). Thus, we interpreted our observations as indication of lower hepatic lipid biosynthesis or secretion in MastitisPost vs. Control cows at calving in response to acute inflammation and lower intestinal lipid absorption.

Noteworthy is that greater decreases with calving and in MastitisPost vs. Control cows were observed in fully or partly deacylated PL metabolites than in PL itself. As a result, LPC to PC ratio and LPE to PE ratio were lower in MastitisPost vs. Control cows at calving. The results suggest that phospholipase or acyltransferase activity of the Lands Cycle may be affected by mastitis infections. In support, pathogenic bacteria and infection have been reported to inhibit phospholipase activity (Hailemariam et al., 2014). In humans, the LPC to PC ratio has been proposed as inflammation marker; for example, lower LPC to PC ratios were associated with increased risk of mortality in sepsis patients (Drobnik et al., 2003). Thus, decreases in LPC to PC ratio and LPE to PE ratio may indicate an acute CM infection in dairy cows, as pathogenic bacteria alter PL metabolism.

CONCLUSIONS

In this study, we describe and evaluate a novel analytical workflow, which is suitable for comprehensive global lipidomics and metabolomics profiling of biological specimen. The observed shifts in serum metabolic, lipidomic, and inflammation profile suggest metabolic crosstalk between mammary gland, muscle, adipose tissue, liver, intestine, and pathogenic bacteria to adapt to parturition and an infectious challenge, which will be the objective of future research. Based on the observed shifts, we propose a time sequence of events potentially preceding and following naturally occurring CM during the close-up period. Early mammary gland development, pregnancy-associated cholestasis, chronic inflammation, elevated choline metabolism, mitochondrial dysfunction, and depleted antioxidant reserves preceded CM and are potential risk factors of CM. Serum markers of acute inflammation followed by elevated adipocyte lipolysis and decreased lipid and bile synthesis, secretion or recycling may follow CM infection and potentially indicate early subclinical stages of CM. Further studies are required to validate and quantify this proposed risk factors and indicators and determine whether these changes are specific to CM or also occur with other diseases.

Supplementary Material

Refer to Web version on PubMed Central for supplementary material.

ACKNOWLEDGMENTS

This study was supported by Oregon State University (Corvallis, OR), the Oregon State University Agricultural Research Foundation (Corvallis, OR), the Oregon Beef Council (Portland, OR), Diamond V (Cedar Rapids, IA), and the E.R. Jackman Internship Support Program. The procurement of the Waters Synapt G2 system was made possible by NIH grant S10RR025628 and funds from the Oregon State University's Research Equipment Reserve Fund. The authors wish to acknowledge the owners and staff of VanBeek Dairy for use of their facilities and their animals; and S. Bledsoe, B. Block, B. Bronson, M. Keller, M. McGuire, P. Ramsing, A. Rudolph, D. Sabedra, C. Sause, C. Shriver-Munsch, M. Swearingen, and E. Zaworski for their assistance with sample collection and data entry.

REFERENCES

Bannerman DD, Rinaldi M, Vinyard BT, Laihia J, and Leino L. 2009 Effects of intramammary infusion of cis-urocanic acid on mastitis-associated inflammation and tissue injury in dairy cow. Am. J. Vet. Res 70:373–382. [PubMed: 19254150]

Bobe G, Young JW, and Beitz DC. 2004 Invited review: pathology, etiology, prevention, and treatment of fatty liver in dairy cows. J. Dairy Sci 87:3105–3124. [PubMed: 15377589]

Broadhurst DI, and Kell DB. 2007 Statistical strategies for avoiding false discoveries in metabolomics and related experiments. Metabolomics 2:171–196.

Ten Bruggencate SJ, Bovee-Oudenhoven IM, Feitsma AL, van Hoffen E, and Schoterman MH. 2014 Functional role and mechanisms of sialyllactose and other sialylated milk oligosaccharides. Nutr. Rev 72:377–389. [PubMed: 24828428]

Danne O, Lueders C, Storm C, Frei U, and Möckel M. 2007 Whole blood choline and plasma choline in acute coronary syndromes: prognostic and pathophysiological implications. Clin. Chim. Acta 383:103–109. [PubMed: 17553478]

Dervishi E, Zhang G, Hailemariam D, Dunn SM, and Ametaj BN. 2015 Innate immunity and carbohydrate metabolism alterations precede occurrence of subclinical mastitis in transition dairy cows. J. Anim. Sci. Technol 57:46. [PubMed: 26705479]

Dervishi E, Zhang G, Dunn SM, Mandal R, Wishart DS, and Ametaj BN. 2016 GC–MS metabolomics identifies metabolite alterations that precede subclinical mastitis in the blood of transition dairy cows. J. Proteome Res 16:433–446. [PubMed: 28152597]

Drackley JK 1999 Biology of dairy cows during the transition period: the final frontier? J. Dairy Sci 82:2259–2273. [PubMed: 10575597]

Drobnik W, Liebisch G, Audebert F-X, Frohlich D, Gluck T, Vogel P, Rothe G, and Schmitz G. 2003 Plasma ceramide and lysophosphatidylcholine inversely correlate with mortality in sepsis patients. J. Lipid Res 44:754–761. [PubMed: 12562829]

Ducker GS, and Rabinowitz JD. 2017 One-carbon metabolism in health and disease. Cell Metab 25:27–42. [PubMed: 27641100]

Eberhardt R 1996 Current concepts of bovine mastitis 4th ed. National Mastitis Council, Arlington VA.

Edmonson A, Lean I, Weaver L, Farver T, and Webster G. 1989 A body condition scoring chart for Holstein dairy cows. J. Dairy Sci 72:68–78.

Ejigu BA, Valkenborg D, Baggerman G, Vanaerschot M, Witters E, Dujardin J-C, Burzykowski T, and Berg M. 2013 Evaluation of normalization methods to pave the way towards large-scale LC-MS-based metabolomics profiling experiments. OMICS 17:473–485. [PubMed: 23808607]

Fadden AN, and Bobe G. 2015 Serum visfatin is a predictive indicator of retained placenta and other diseases in dairy cows. J Vet. Sci. Med. Diagn 5:1–6.

Franceschi C, Capri M, Monti D, Giunta S, Olivieri F, Sevini F, Panagiota Panourgia M, Invidia L, Celani L, Scurti M, Cavenini E, Castellani GC, and Salvioli S. 2007 Inflammaging and anti-inflammaging: a systemic perspective on aging and longevity emerged from studies in humans. Mech. Ageing Dev 128:92–105. [PubMed: 17116321]

Geenes V, and Williamson C. 2009 Intrahepatic cholestasis of pregnancy. World J. Gastroenterol 15:2049–2066. [PubMed: 19418576]

Gopal PK, and Gill HS. 2000 Oligosaccharides and glycoconjugates in bovine milk and colostrum. Br. J. Nutr 84:S69–S74. [PubMed: 11242449]

Gray RG, Kousta E, McCarthy MI, Godsland IF, Venkatesan S, Anyaoku V, and Johnston DG. 2013 Ethnic variation in the activity of lipid desaturases and their relationships with cardiovascular risk factors in control women and an at-risk group with previous gestational diabetes mellitus: a cross-sectional study. Lipids Health Dis 12:25. [PubMed: 23496836]

Griffith OW 1987 Mammalian sulfur amino acid metabolism: an overview. Methods Enzymol 143:366–376. [PubMed: 3309559]

Gruys E, Toussaint MJM, Upragarin N, Van EA, Adewuyi AA, Candiani D, Nguyen TK, and Sabeckiene J. 2005 Acute phase reactants, challenge in the near future of animal production and veterinary medicine. J. Zhejiang Univ. Sci. B 6:941–947. [PubMed: 16187407]

Hailemariam D, Mandal R, Saleem F, Dunn SM, Wishart DS, Ametaj BN, Yokomizo Y, Kreutz M, Fonsmark L, Madsen PL, and Klarlund P. 2014 Identification of predictive biomarkers of disease state in transition dairy cows. J. Dairy Sci 97:2680–2693. [PubMed: 24630653]

Huber K, Dänicke S, Rehage J, Sauerwein H, Otto W, Rolle-Kampczyk U, and von Bergen M. 2016 Metabotypes with properly functioning mitochondria and anti-inflammation predict extended productive life span in dairy cows. Sci. Rep 6:24642. [PubMed: 27089826]

Hurley WL, and Theil PK. 2011 Perspectives on immunoglobulins in colostrum and milk. Nutrients 3:442–474. [PubMed: 22254105]

Imhasly S, Bieli C, Naegeli H, Nyström L, Ruetten M, and Gerspach C. 2015 Blood plasma lipidome profile of dairy cows during the transition period. BMC Vet. Res 11:252. [PubMed: 26446667]

Ingvartsen KL 2006 Feeding- and management-related diseases in the transition cow: physiological adaptations around calving and strategies to reduce feeding-related diseases. Anim. Feed Sci. Technol 126:175–213.

Kelton DF, Lissemore KD, and Martin RE. 1998 Recommendations for recording and calculating the incidence of selected clinical diseases of dairy cattle. J. Dairy Sci 81:2502–2509. [PubMed: 9785242]

Kessler EC, Gross JJ, Bruckmaier RM, and Albrecht C. 2014 Cholesterol metabolism, transport, and hepatic regulation in dairy cows during transition and early lactation. J. Dairy Sci 97:5481–5490. [PubMed: 24952770]

Kirkwood JS, Maier C, and Stevens JF. 2013 Simultaneous, untargeted metabolic profiling of polar and nonpolar metabolites by LC-Q-TOF mass spectrometry. Curr. Protoc. Toxicol Chapter 4:Unit4.39.

Kontush A, Lhomme M, and Chapman MJ. 2013 Unraveling the complexities of the HDL lipidome.. J. Lipid Res 54:2950–2963. [PubMed: 23543772]

Koves TR, Ussher JR, Noland RC, Slentz D, Mosedale M, Ilkayeva O, Bain J, Stevens R, Dyck JRB, Newgard CB, Lopaschuk GD, and Muoio DM. 2008 Mitochondrial overload and incomplete fatty acid oxidation contribute to skeletal muscle insulin resistance. Cell Metab 7:45–56. [PubMed: 18177724]

Kuhla B, Nürnberg G, Albrecht D, Görs S, Hammon HM, and Metges CC. 2011 Involvement of skeletal muscle protein, glycogen, and fat metabolism in the adaptation on early lactation of dairy cows. J. Proteome Res 10:4252–4262. [PubMed: 21774562]

Lai IH, Tsao JH, Lu YP, Lee JW, Zhao X, Chien FL, and Mao SJ. 2009 Neutrophils as one of the major haptoglobin sources in mastitis affected milk. Vet. Res 40:17. [PubMed: 19094922]

Lammert F, Marschall HU, Glantz A, and Matern S. 2000 Intrahepatic cholestasis of pregnancy: molecular pathogenesis, diagnosis and management. J. Hepatol 33:1012–1021. [PubMed: 11131439]

Lee YS, Cho Y, and Shin M-J. 2015 Dietary very long chain saturated fatty acids and metabolic factors: findings from the Korea National Health and Nutrition Examination Survey 2013. Clin. Nutr. Res 4:182–189. [PubMed: 26251837]

Lin Z, Zhang Z, Lu H, Jin Y, Yu L, and Liang Y. 2014 Joint MS-based platforms for comprehensive comparison of rat plasma and serum metabolic profiling. Biomed. Chromatogr 28:1235–1245. [PubMed: 24619916]

López-Otín C, Blasco MA, Partiridge L, Serrano M, and Kroemer G. 2013 The hallmarks of aging. Cell 153:1194–1217. [PubMed: 23746838]

MacKenzie DDS, and Lascelles AK. 1968 The transfer of [131I]-labelled immunoglobulins and serum albumin from blood into milk of lactating ewes. Aust. J. Exp. Biol. Med. Sci 46:285–294. [PubMed: 5692800]

Malik VS, Chiuve SE, Campos H, Rimm EB, Mozaffarian D, Hu FB, and Sun Q. 2015 Circulating very-long chain saturated fatty acids and incident coronary heart disease in U.S. men and women. Circulation 132:260–268. [PubMed: 26048094]

Mansor R, Mullen W, Albalat A, Zerefos P, Mischak H, Barrett DC, Biggs A, and Eckersall PD. 2013 A peptidomic approach to biomarker discovery for bovine mastitis. J. Proteomics 85:89–98. [PubMed: 23639846]

Moyes KM, Larsen T, and Ingvartsen KL. 2013 Generation of an index for physiological imbalance and its use as a predictor of primary disease in dairy cows during early lactation. J. Dairy Sci 96:2161–2170. [PubMed: 23403197]

Nakamura T, Kawase H, Kimura K, Watanabe Y, Ohtani M, Arai I, and Urashima T. 2003 Concentrations of sialyloligosaccharides in bovine colostrum and milk during the prepartum and early lactation. J. Dairy Sci 86:1315–1320. [PubMed: 12741556]

National Research Council (NRC). 2001 Nutrient Requirements of Dairy Cattle 7th rev. ed. National Acad. Sci, Washington, DC

Qu Y, Lytle K, Traber MG, and Bobe G. 2013 Depleted serum vitamin E concentrations precede left displaced abomasum in early-lactation dairy cows. J. Dairy Sci 96:3012–3022. [PubMed: 23497999]

Qu Y, Fadden AN, Traber MG, and Bobe G. 2014 Potential risk indicators of retained placenta and other diseases in multiparous cows. J. Dairy Sci 97:4151–4165. [PubMed: 24792789]

Rollin E, Dhuyvetter KC, and Overton MW. 2015 The cost of clinical mastitis in the first 30 days of lactation: an economic modeling tool. Prev. Vet. Med 122:257–264. [PubMed: 26596651]

Rukkwamsuk T, Geelen MJH, Kruip TAM, and Wensing T. 2000 Interrelation of fatty acid composition in adipose tissue, serum, and liver of dairy cows during the development of fatty liver postpartum. J. Dairy Sci 83:52–59. [PubMed: 10659963]

Servillo L, Giovane A, Cautela D, Castaldo D, and Balestrieri ML. 2014 Where does N(ε)-trimethyllysine for the carnitine biosynthesis in mammals come from? PloS ONE 9:e84589. [PubMed: 24454731]

Sharma N, Singh NK, and Bhadwal MS. 2011 Relationship of somatic cell count and mastitis: an overview. Asian-Aust. J. Anim. Sci 24:429–438..

Silbernagel G, Kovarova M, Cega A, Machann J, Schick F, Legmann R, Häring HU, Stefan N, Schlecher E, Fritsche A, and Peter A. 2012 High heptaic SCD1 activity is associated with low liver fat content in healthy subjects under a lipogenic diet. J. Clinc. Endocrinol. Metab 97:E2288–E2292.

Sordillo LM, Contreras GA, and Aitken SL. 2009 Metabolic factors affecting the inflammatory response of periparturient dairy cows.. Anim. Health Res. Rev 10:53–63.. [PubMed: 19558749]

Stefan N, Peter A, Cega A, Staeger H, Machann J, Schick F, Claussen CD, Fritsche A, Häring HU, and Schleicher E. 2008 Low heaptic stearoyl-CoA desaturase 1 activity is associated with fatty liver and insulin resistance in obese humans. Diabetologia 51:648–656. [PubMed: 18286258]

Sundekilde UK, Poulsen NA, Larsen LB, and Bertram HC. 2013 Nuclear magnetic resonance metabonomics reveals strong association between milk metabolites and somatic cell count in bovine milk. J. Dairy Sci 96:290–299. [PubMed: 23182357]

Tai CC, and Ding ST. 2010 N-3 polyunsaturated fatty acids regulate lipid metabolism through several inflammation mediators: mechanisms and implications for obesity prevention. J. Nutr. Biochem 21:357–363. [PubMed: 20149625]

Tao N, DePeters EJ, German JB, Grimm R, and Lebrilla CB. 2009 Variations in bovine milk oligosaccharides during early and middle lactation stages analyzed by high-performance liquid chromatography-chip/mass spectrometry. J. Dairy Sci 92:2991–3001. [PubMed: 19528576]

Thomas FC, Mudaliar M, Tassi R, McNeilly TN, Burchmore R, Burgess K, Herzyk P, Zadoks RN, and Eckersall PD. 2016 Mastitomics, the integrated omics of bovine milk in an experimental model of Streptococcus uberis mastitis: 3. untargeted metabolomics. Mol. BioSyst 12:2762–2769. [PubMed: 27412568]

USDA. 2009 Dairy 2007, Part V: Changes in Dairy Cattle Health and Mangagement Practices in the Uniteed States, 19960207 USDA:APHIS:VS, CEAH. Fort Collins, CO.

Viguier C, Arora S, Gilmartin N, Welbeck K, O'Kennedy R, and O'Kennedy R. 2009 Mastitis detection: current trends and future perspectives. Trends Biotechnol 27:486–493. [PubMed: 19616330]

Wang Y-D, Chen W-D, Wang M, Yu D, Forman BM, and Huang W. 2008 Farnesoid X receptor antagonizes nuclear factor kappa B in hepatic inflammatory response. Hepatology 48:1632–1643. [PubMed: 18972444]

Xi X, Kwok L-Y, Wang Y, Ma C, Mi Z, and Zhang H. 2017 Ultra-performance liquid chromatography-quadrupole-time of flight mass spectrometry MS E-based untargeted milk metabolomics in dairy cows with subclinical or clinical mastitis. J. Dairy Sci 100:4884–4896. [PubMed: 28342601]

Xia J, Mandal R, Sinelnikov IV, Broadhurst D, and Wishart DS. 2012 MetaboAnalyst 2.0-a comprehensive server for metabolomic data analysis. Nucleic Acids Res 40:W127–W133. [PubMed: 22553367]

Yan J, Jiang X, West AA, Perry CA, Malysheva OV, Devapatla S, Pressman E, Vermeylen F, Stabler SP, Allen RH, and Caudill MA. 2012 Maternal choline intake modulates maternal and fetal biomarkers of choline metabolism in humans. Am. J. Clin. Nutr 95:1060–1071. [PubMed: 22418088]

Yu Z, Kastenmüller G, He Y, Belcredi P, Möller G, Prehn C, Mendes J, Wahl S, Roemisch-Margl W, Ceglarek U, Polonikov A, Dahmen N, Prokisch H, Sie L, Li Y, Wichmann H-E, Peters A, Kronenberg F, Suhre K, Adamski J, Illig T, and Wang-Sattler R. 2011 Differences between human plasma and serum metabolite profiles. PLoS ONE 6:e21230. [PubMed: 21760889]

Zhang G, Dervishi E, Dunn SM, Mandal R, Liu P, Han B, Wishart DS, and Ametaj BN. 2017 Metabotyping reveals distinct metabolic alterations in ketotic cows and identifies early predictive serum biomarkers for the risk of disease. Metabolomics 13:43.

Zhou Z, Garrow TA, Dong Z, Luchini DN, and Loor JJ. 2017 Hepatic activity and transcription of betaine-homocystein methyltransferase, methionine synthase, and cystathionine synthase in periparturient dairy cows are altered to different extents by methionine and choline. J. Nutr 147:11–19. [PubMed: 27881594]

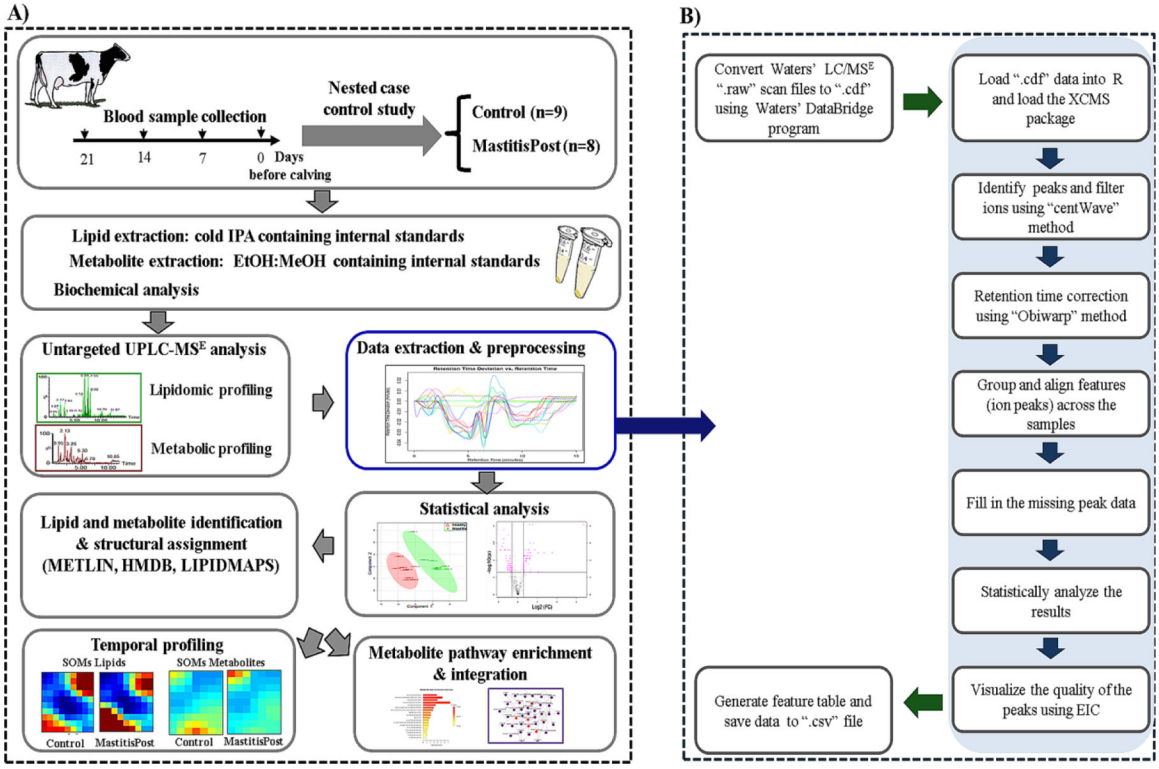

Figure 1.

A) Experimental workflow of untargeted metabolomic, lipidomic, and biochemical analyses for predictive biomarker discovery of bovine clinical mastitis during the close-up period (21, 14, 7, and 0 days before calving), and B) data pre-processing pipeline using the XCMS package in R (EIC: extracted ion chromatogram) (more details provided in Table S5).

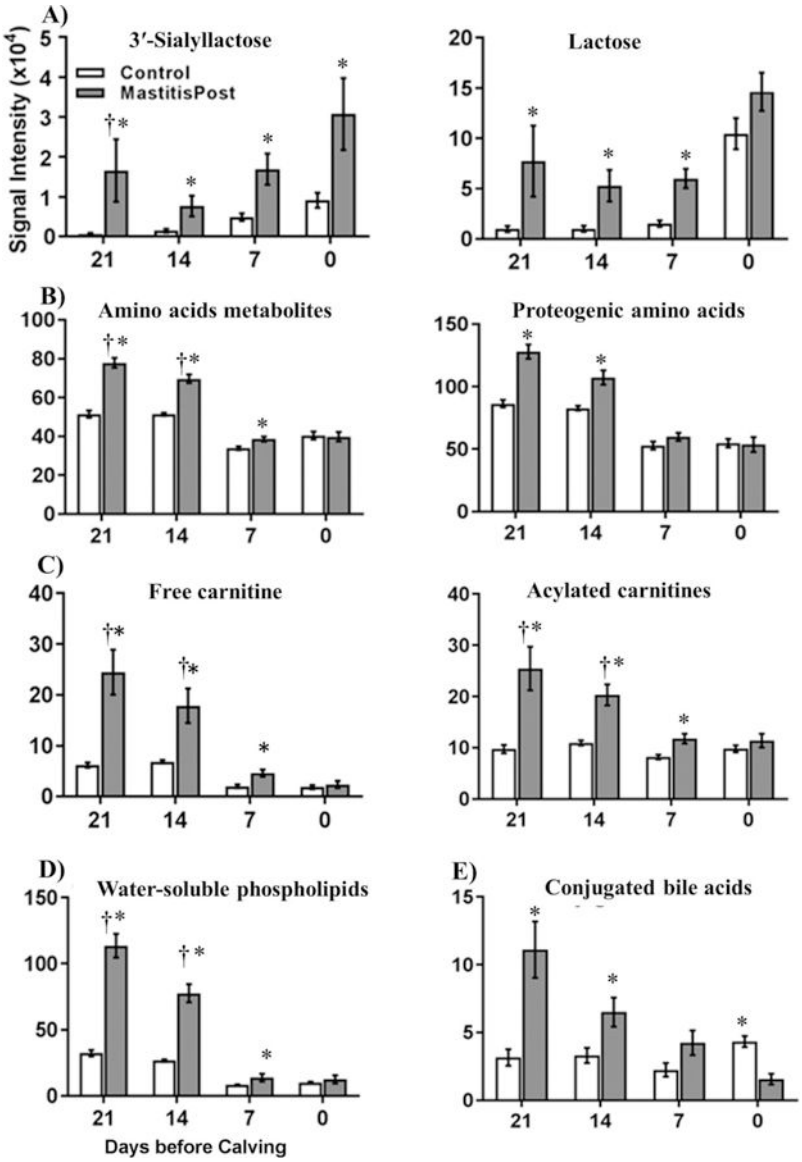

Figure 2.

Summed serum signal intensities (mean ± SEM) of A) 3'-sialyllactose and lactose, B) amino acid metabolites and proteogenic amino acids, C) free and acylated carnitines, D) water-soluble phospholipids, and E) conjugated bile acids in serum of MastitisPost (n=8) and Control (n=9) cows at 21, 14, 7, and 0 days before calving. Crosses indicated complete group separation (AUC-ROC = 1), and asterisks indicate significant ($p < 0.05$) group differences between MastitisPost and Control cows using Wilcoxon rank sum test.

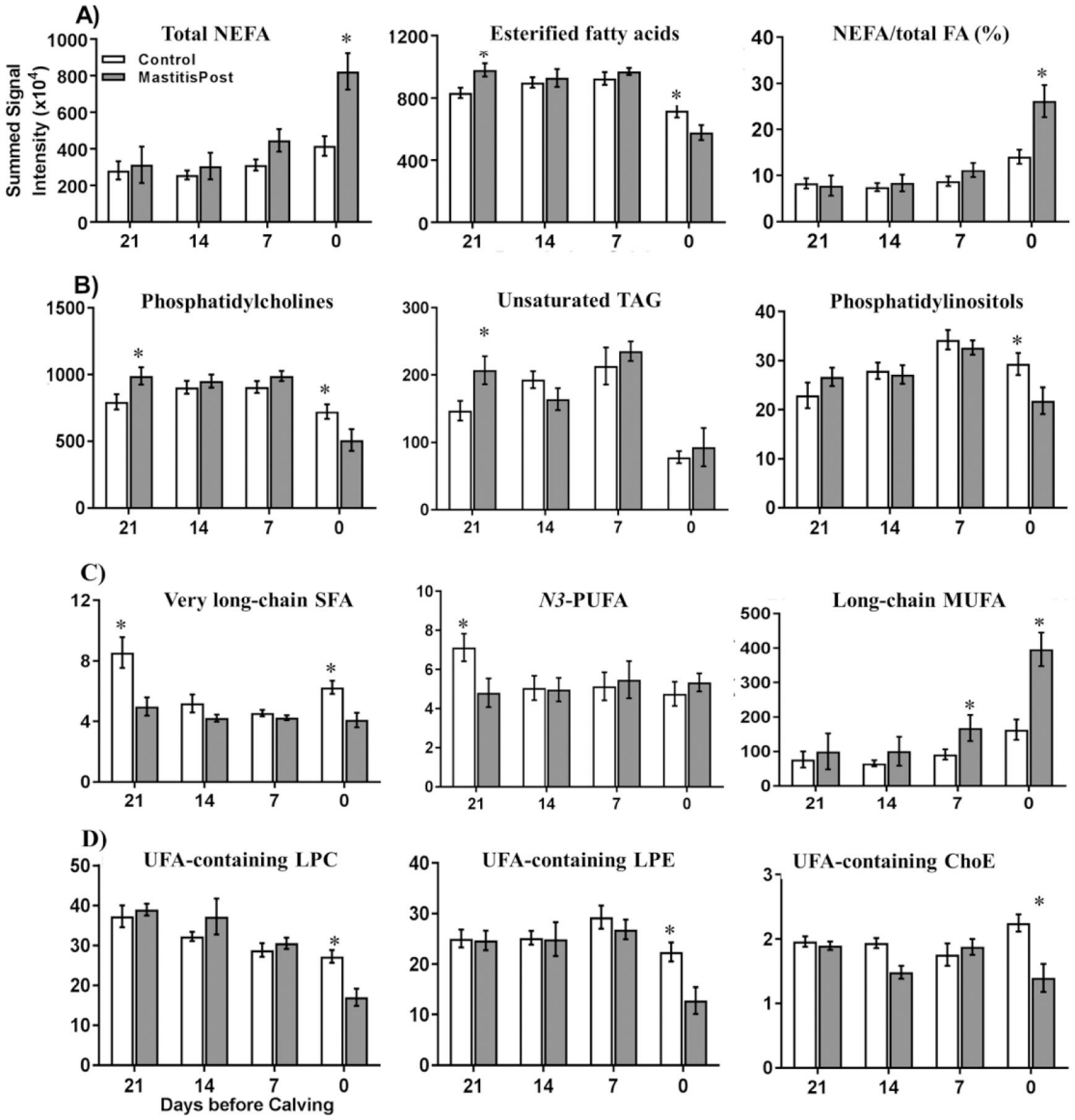

Figure 3.

Summed serum signal intensities (mean ± SEM) of total A) NEFA, esterified fatty acids, and %NEFA (proportion of esterified FA on total FA, B) phosphatidylcholine, unsaturated TAG, and phosphatidylinositols, C) very long-chain SFA and *N3*-PUFA, and long-chain MUFA, and D) UFA-containing LPC, LPE, and cholesteryl esters in serum of MastitisPost (n=8) and Control (n=9) cows at 21, 14, 7, and 0 days before calving. Asterisks indicate significant ($p \leq 0.05$) group differences between MastitisPost and Control cows using Wilcoxon rank sum test.

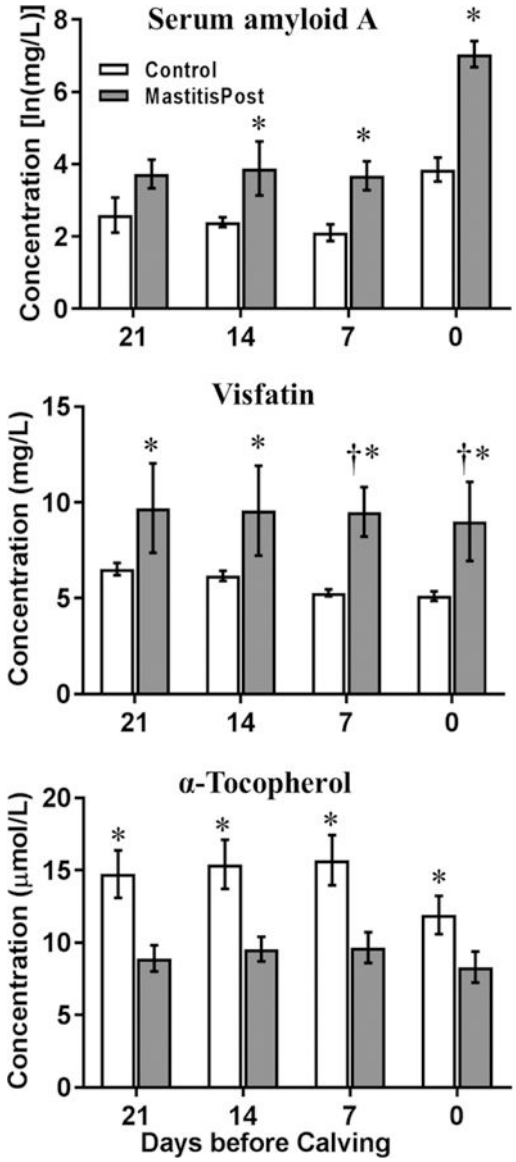

Figure 4.

Serum concentrations (mean ± SEM) of serum amyloid A, visfatin, and α-tocopherol measured using biochemical analysis at 21, 14, 7, and 0 days before calving. Crosses indicated complete group separation (AUC-ROC = 1), and asterisks show significant ($p \leq 0.05$) differences between MastitisPost (n=8) and Control (n=9) cows using Wilcoxon rank sum test.

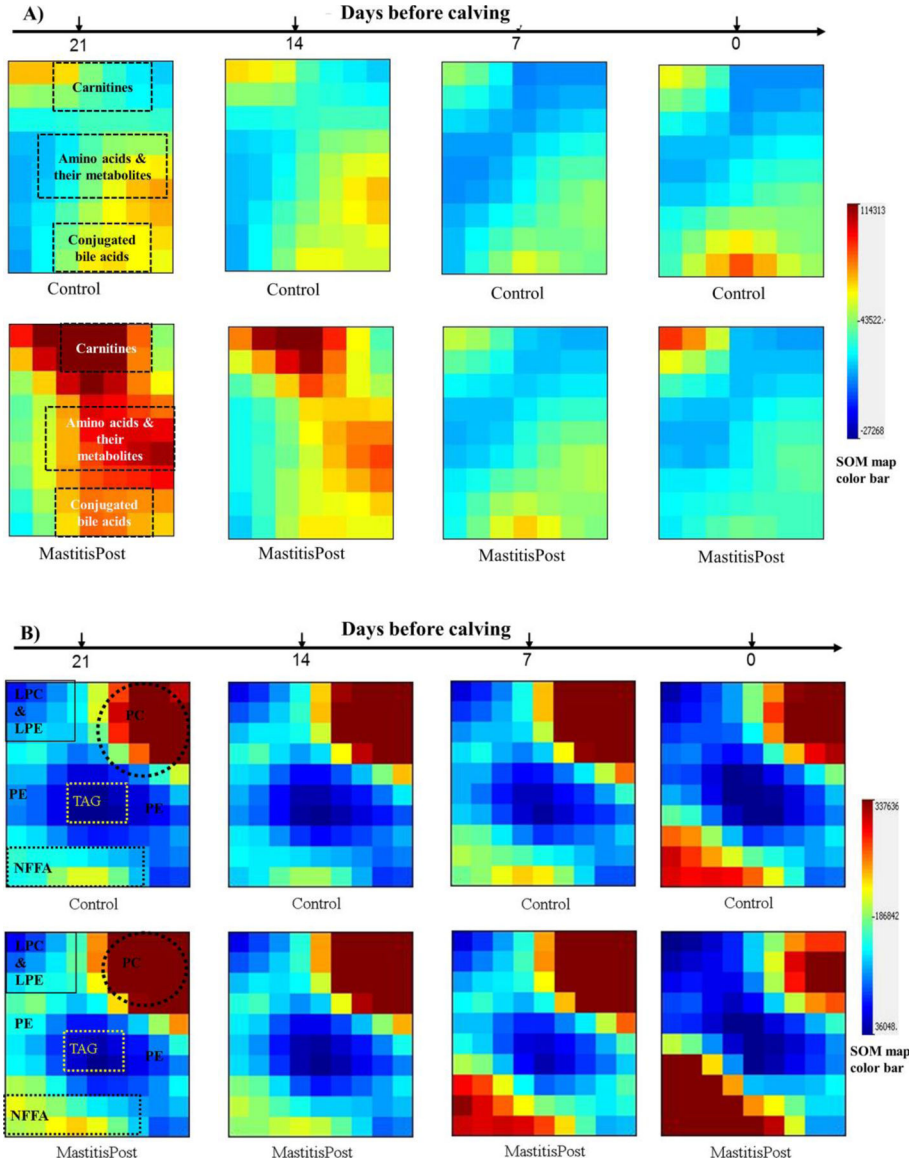

Figure 5.

Self-organizing maps (SOM) of MastitisPost and Control cows A) metabolomic and B) lipidomic at 21, 14, 7, and 0 days before calving are visualized in Gene Expression Dynamics Inspector (GEDI).

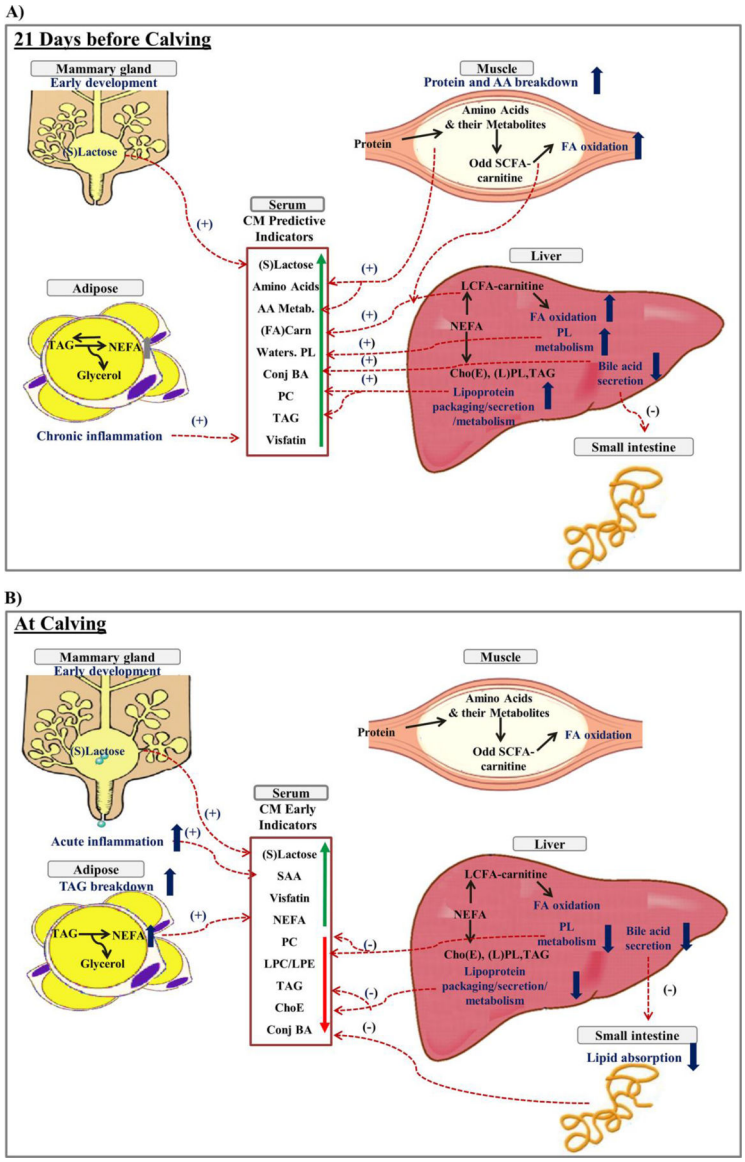

Figure 6.

Schematic representation of proposed cross-talk between mammary gland, adipose tissue, muscle, liver, small intestine, and pathogenic bacteria in MastitisPost vs. Control cows A) at 21 days before calving and B) at calving. Proposed processes and their differences between MastitisPost vs. Control cows in tissue are in dark blue. Dashed lines with plus signs (+) indicate higher and minus signs (−) indicate lower signal intensities in serum in MastitisPost vs. Control cows. Abbreviation key: ChoE: cholesteryl esters; ConjBA: conjugated bile acids; FA (Carn): free and acylated carnitines; LCFA-carnitine: long-chain acylated carnitines; LPL: lysophospholipids (LPE and LPC); NEFA: non esterified fatty acids; PL: phospholipids [phosphotidylcholines (PC) and phosphotidylethanolamine (PE)]; Odd SCFA-carnitine: short-chain odd acylated carnitines; serum amyloid A (SAA); (S)lactose: (3'-sialyllactose and lactose); TAG: triacylglycerol; and water-soluble PL: water soluble phospholipids.

Table 1.

List of putatively identified metabolites and lipids that could accurately discriminate all MastitisPost (n=8) cows from Control (n=9) cows at ≥1 sampling time (AUC-ROC = 1) or with significant ($p < 0.05$) group differences at ≥3 sampling times

Metabolite/Lipid class	Metabolite/Lipid	Fold-change (M/C in %)				*p*-value (group differences)[1]			
		Days before calving				Days before calving			
		21	14	7	0	21	14	7	0
Mammary gland-derived carbohydrates	3'-Sialyllactose	1,440	306	156	125	0.0005	0.01	0.008	0.03
	Lactose	855	487	229	77	0.007	0.01	0.001	0.07
Amino acid metabolites	Total	43	30	8	−3	0.0005	0.0005	0.01	0.77
	Trimethyl-lysine	145	71	27	−17	0.0005	0.0005	0.05	0.63
	Methyl-histidine	187	108	29	6	0.0005	0.007	0.10	0.56
	Asymetric dimethylarginine	129	87	26	−35	0.0005	0.001	0.08	0.44
	Creatine	124	154	29	12	0.0005	0.001	0.05	0.50
	Hippuric acid	72	51	32	−43	0.02	0.002	0.34	0.005
Proteinogenic amino acids	Total	53	35	3	−8	0.0008	0.003	0.21	0.44
	Tyrosine	127	95	19	−27	0.0005	0.0005	0.25	0.70
	Histidine	78	47	6	55	0.0005	0.005	0.34	0.03
	Phenylalanine	92	46	10	−16	0.0005	0.0008	0.10	0.63
	Threonine	87	29	31	12	0.0005	0.03	0.10	0.92
	Proline	79	77	54	−10	0.0005	0.0005	0.007	0.63
Water-soluble phospholipid metabolites	Total	255	183	−35	−1	0.0005	0.0005	0.003	0.92
	Methyl ethanolamine phosphate	526	145	72	−42	0.0005	0.0005	0.05	0.56
	Choline	439	298	68	70	0.0005	0.0005	0.08	0.15
	Phosphorylcholine	65	50	17	−18	0.0005	0.0005	0.07	0.50
	Betaine	55	45	23	−19	0.007	0.001	0.03	0.77
Free and acylated carnitines	Total	195	106	55	6	0.0005	0.0005	0.002	0.77
	Free carnitine	226	117	87	0	0.0005	0.0005	0.002	0.70
	Car C3:0	561	208	114	−27	0.0005	0.001	0.02	0.21
	Car C10:0	40	36	12	0	0.0005	0.001	0.29	0.70
	Car C18:1	591	323	179	27	0.0008	0.005	0.03	0.25
Conjugated bile acids	Total	239	83	113	−69	0.004	0.009	0.07	0.002
	Taurolithocholic acid	56	−30	36	−60	0.92	0.63	0.12	0.0005
	Taurocholic acid	436	133	65	−57	0.009	0.002	0.21	0.009
	Glycodeoxycholic acid	415	150	78	−67	0.004	0.02	0.04	0.001
	Glycocholic acid	240	59	58	−67	0.004	0.03	0.07	0.005
Vitamins and cofactors	Niacinamide	120	83	1	−44	0.0005	0.05	0.5	0.34
	α-tocopherol	−35	−35	−24	−19	0.004	0.007	0.02	0.05

Metabolite/Lipid class	Metabolite/Lipid	Fold-change (M/C in %)				*p*-value (group differences)[1]			
		Days before calving				Days before calving			
		21	14	7	0	21	14	7	0
Inflammation markers	Total	175	234	242	1,914	0.18	0.001	0.001	0.0005
	Serum Amyloid A	452	465	307	3,870	0.12	0.05	0.005	0.0008
	Visfatin	45	54	82	63	0.0011	0.0008	0.0005	0.0005
Phosphatidylcholine	PC(16:0/16:1)	83	26	40	1	0.04	0.03	0.02	0.77
Triacylglycerol	TAG(16:0/18:0/18:1)	39	−16	6	−77	0.02	0.03	0.39	0.04

[1]Sampling times with AUC-ROC > 0.90 have a $p \leq 0.005$ and those with complete group separation (AUC-ROC = 1) have a $p = 0.0005$.